Pro Index | Journal of Science in Medicine and Life
Volume: 2 Issue: 10 Year: 2024
ISSN: 2992-9202 | http://journals.proindex.uz

Design, Implementation, and Studying Efficiency of Peristaltic Pumps Roller for Kidney Failure

Saisban Lateef finjan, Abu al-Hassan Abd al-Wahhab Jabr,
Lec. Dr. Suhair Mohammed Hassan, Ass. Lec. Huda Farooq Jam
Republic of Iraq, Ministry of Higher Education and Scientific Research,
Middle Technical University, Electrical Engineering Technical College

Abstract: The purpose of this project is to Design, implementation, and studying efficiency of peristaltic pumps roller for kidney failure. Outcomes of the design process involves, learning how to design and how to successfully design and implement of the system. The project system consists of switching power supply 5VDC 4A DC and L298N motor drive controller board module dual h Bridge DC Bipolar stepper motor. Safety unit is performed by using air bubble sensor which is used to stop the motor in case of bubble insertion. The IR sensor used which is consists of photo diode and photo transistor to detect the bubble and these components are connected to LM358 operation amplifier to detect bubble, stop motor and alarm user at the same time by the buzzer in ON state. Software of PIC12F675 is used as a microcontroller designed to control speed of motor driver and to stop motor in case of air bubble passing. The Performance of project system is experimentally tested by sensitivity and overall accuracy evaluation depending upon the classification models of true positive [TP], false positive [FP], true negative [TN], and false negative [FN]. Values of 99% sensitivity and 98.5% of overall accuracy are reflected to high efficiency in fabrication process of project system.

Key points: Process, Organization, Europe, modern, trend, country.

CHAPTER 1 INTRODUCTION

1.1 Introduction

Roller pumps have been widely used in the ventricular assist field for many years, while the significant hemolysis caused by its mechanical stress is still a fundamental problem. Although the usual under-occlusion setting was considered as an effective method to reduce the hemolysis rate, its non-occlusive condition of the whole process may cause serious backflow results, which exactly places many restrictions on this method. The peristaltic pump generated high pressure and flow pulses due to the interaction between the roller and the tube. The squeezing and relaxing of the tube during the operative phase allowed the liquid to have a pulsatile behavior.

For low pressure fluid transport applications often require low and precise volumetric flow rates that including low leakage to reduce additional costly and complex sensors. A peristaltic pump design was realized, with the fluid's flexible transport channel formed by a solid cavity and a wobbling plate comprising a rigid and a soft layer. A thorough characterization of the pump system is required to design and dimension the components of the peristaltic pump. To capture all these parameters and their dependencies on various operation-states, often complex and long-lasting dynamic 3D simulations are required.

Roller pump is the pump console generally consists of numerous pumps that rotate motors and that "massage" tubes peristaltically. This motion drives the blood softly through the tube. The term roller

pump or peristaltic pump is usually referred to. The pumps are cheaper than the centrifugal components but are likely to over-pressure if the lines are tightened up or bent. The report was published.

They will also generate a large air embolism and require the per-fusionist to monitor them constantly and closely. Figure 1.1 Illustrate the five and four rollers.

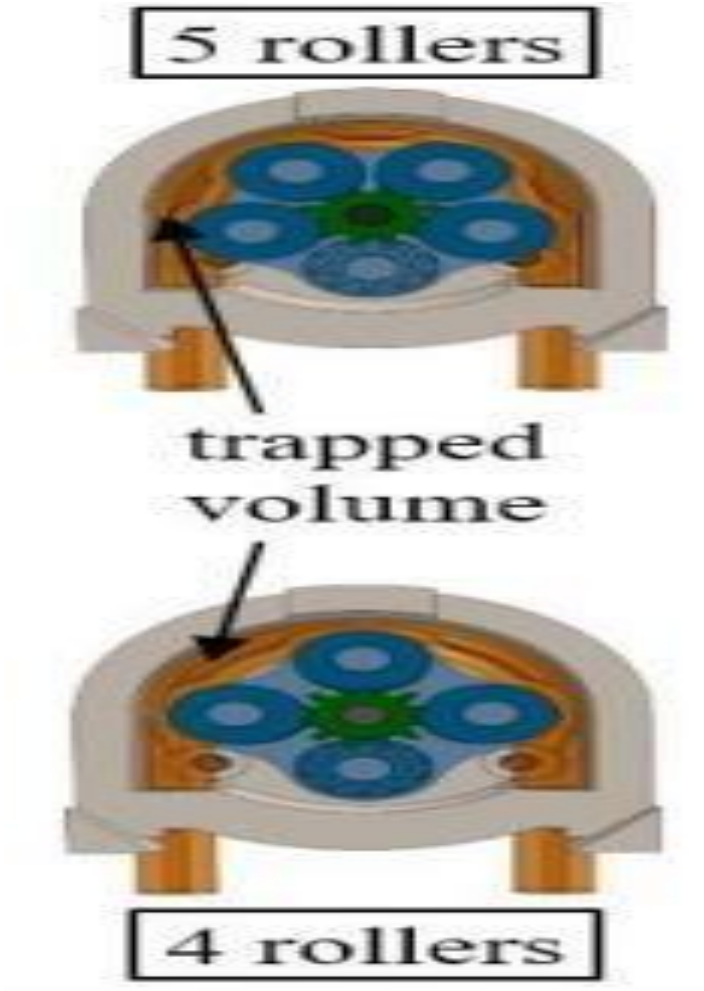

Figure 1.1 Illustrate the five and four rollers.

CHAPTER 2 THEORETICAL BACKGROUND

2. Introduction

2.1. A systematic review of the literature

The systematic literature review to answer the research question was performed as daily life activities (DLAs) are necessary for quality of life so a lot of features allow users to enjoy their life with good health. The systematic review has been achieved with A biomimetic circular pump was created to move a wide range of Newtonian and non-Newtonian fluids with different viscosities in an effortless, silent, and secure manner. Eight silicone-dependent pneumatic circle actuators with elliptical inside conduit longitudinal diameters of 2 cm operate the system. Investigations were done into how different peristaltic actuator patterns and frequencies affected the flow rate attained. The findings show that the flexible and elastic silicone-dependent self-priming peristaltic pump designed may attain flow rates exceeding 250 l/h and could be used as a substitute for traditional technical devices in the field of electro-mobility [1]. The analysis of various proposed pump models revealed some versions that can eliminate pulsation and thus dosage errors. The study examined a few pump designs and put them through flow experiments to determine how volume changed in response to pulsation. In order to evaluate two pumps made for this purpose and obtain continuous

flow, the use of a manometer and a series of vertical tubes was suggested. The utilization of silicone tubes with thicker or validated walls, which help stop the tube from widening at higher pressures, which happens when the biomaterial has a greater density or the nozzle diameter is small, as well as the printing of 3D models, dimensional lifting of the printed designs, and thorough tests with various biomaterials were all recommended by the author [2]. A comprehensive design approach that takes into account experimental approvals, analytical as well as mathematical calculations, and maximum temperatures and pressures for a peristaltic pump. To determine the necessary drive torque, material information from candidate materials (liquid silicone rubber, acrylonitrile rubber, and thermoplastic elastomer) is immediately applied in an experimental selection procedure. A semi-physical, analytical model for the prediction was created and verified by describing the pump model [3]. An investigation into a more reliable modification form for the occlusion condition was done using simulation experiments of computational fluid dynamics (CFD), and the occlusion angle was proposed. Based on the occlusion incidence and several factors, a roller pump's parameterized geometry was created. The CFD model and the analytical formulae used to estimate the boundary location were introduced to replicate the motion of the roller [4].

Presents a peristaltic rotary pump-based dosing system's construction and characterization. Variations in speed and delay time have no impact on the suggested dosing methods' performance. The average and median values of the dosage resolution also produced results that were well in line with theoretical estimations. This demonstrates the suggested pumps' dependability and accuracy, as well as their adaptability for irregular operation and a range of rotational speed situations[5].An accessible peristaltic pump that may be used with microfluidic systems for point-ofcare testing was built using a combination of three-dimensional printed parts and standard hardware. This pump can generate flow rates of up to 1.6 mL per minute and accepts silicone rubber tubing in sizes ranging from 1.5 to 3 mm. With the use of a microcontroller, this device may be customized to match a variety of tiny volume control functions, such as precise liquid aliquoting, microfluidic flow control, and the generation of physiologically appropriate forces for the study of cellular mechanobiology [6]. The tube was stimulated by a circulating asymmetrical oscillation in a redesigned peristaltic pump. The pump's properties combine continuous flow and adjustable flow pulsation, which set it apart from traditional roller pumps. Compared to a traditional roller pump, the non-occlusive pump may decrease flow pulsation by around 85% while operating in continuous mode. By altering the oscillation magnitude, programmable circulation pulsations could be produced. This control feature makes it possible to create defined volume flow pulses. In the human artery network, for example, a second-generation vessel pulse could be produced experimentally. For in vitro studies of biocompatible encapsulations under physiological flow conditions, certain pulse forms are necessary [7]. The mechanics of two-phase peristaltic flows in an experimental study were presented. The slug size, translational movement, and frequency of the slug movement were measured, and the impact of the liquid rate of flow and liquid superficial velocity was examined. These are the distinctive variables of the twophase pulsatile slug flows. The results demonstrate that the flow rate and liquid surface level velocity increase the average and maximum slug velocities as well as the dominant magnitude of the slug velocity, but it is not possible to establish with certainty a correlation between the liquid surface level velocity and the slug length. The control and warning systems of intelligent dialysis equipment can leverage the measuring approach described in this article [8]. Explains a different modeling approach to the volume concentration, pulsatile flow rate characteristics, and pressure pulsations frequently observed in peristaltic pumps. Instead of concentrating on each particular roller, the model focuses on the flow rate at the pump's input and output. This concept allows for a variable number of rollers and is very scalable. A peristaltic pump that was 3D printed and a flow rate test bench for pulsatile flow are used to validate the model. To validate the model, the pump may handle roller housings with three or two different numbers of rollers [9]. To forecast the fluid flow in a particular peristaltic pump composed of one metallic roller and a hyperelastic tube that pumps a viscous Newtonian fluid, fluid-structure interaction (FSI) modeling was used. It took the coupling of hyperelastic material dynamics and turbulence flow dynamics to adequately characterize the entire physics of the pump. To avoid roller and hose portion pressure peaks, the application of FSI modeling for geometric

pump housing modification was examined. The model enabled analysis of the impact of pump design changes on the flow rate, flow fluctuations, and stress conditions in the tube, including tube occlusion, tube diameter, and roller speed [10]. Explains the experimental characteristics of the design of a linear pneumatic peristaltic actuator that may impose either a force or a displacement between rollers. The design used experimental friction parameters as well as the force between the rollers. It was also determined whether there was any chamber leakage. The development of an experimental third-order linear model identification is the last step [11].

CHAPTER 3 METHODOLOGY

3.1 Introduction

This chapter covers the hardware and software configuration of this study as well as it presents the methodology used to accomplish the work goals. The methodology included in this study is organized into three phases. The first phase is the design and implementation of the system. The second phase is controlling the system by algorithm. The last phase is performance metrics evaluation by optimization of the measurement accuracy for executing orders based on the sensitivity and specificity in addition to the performance accuracy information of the design.

3.2 System Design and Development

This section describes the system design and development of the proposed peristaltic pump.

3.2.1 System design

The proposed system comprises a DC driver, DC motor, roller, microcontroller, and bubbles detectors. Figure 3.1 presents a block diagram of the system. The framework is designed to keep in view any demands for future development and can be simply modified by adding and replacing the input or output parts.

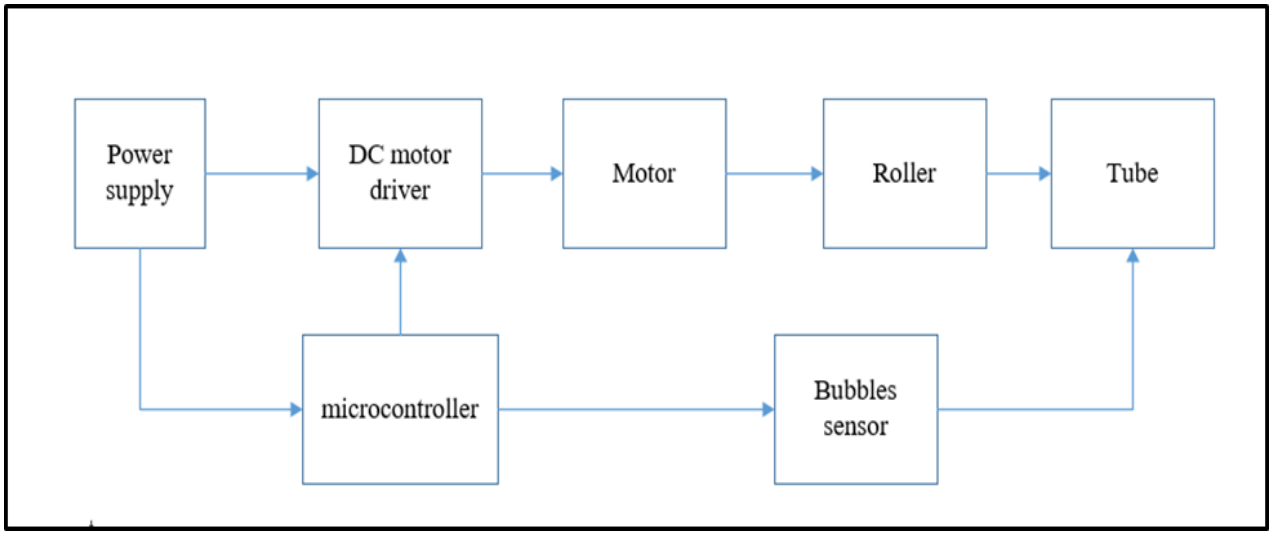

Figure 3.1 Block diagram of the system.

3.3. Hard ware configuration

In this stage, the hardware implementation of the design and implementation of assistive feeding device can be divided into several units as discussed below:

3.3.1 Power supply

Switching power supply 5VDC 4A DC Jack is used in this system as shown in figure 3.2. Which has high power, high current, high stability, safe and reliable[12]. In addition to cost-effective, manufacturers have done multiple protections such as over-current protection and short-circuit protection to ensure that it is safe and reliable.

Figure 3.2 switching power supply[12]

3.3.2 Motor Driver Unit

L298N motor drive controller board module dual h Bridge DC Stepper [13] as shown in figure 3.3. In this system used this driver because it has good specification like logic voltage: 5v, logic current 0ma-36ma, storage temperature: -20 ℃ to ℃ to +135, operating mode: h-bridge driver (dual), drive voltage: 5v-35v, drive current:

2a (max single bridge), and maximum power: 25w.

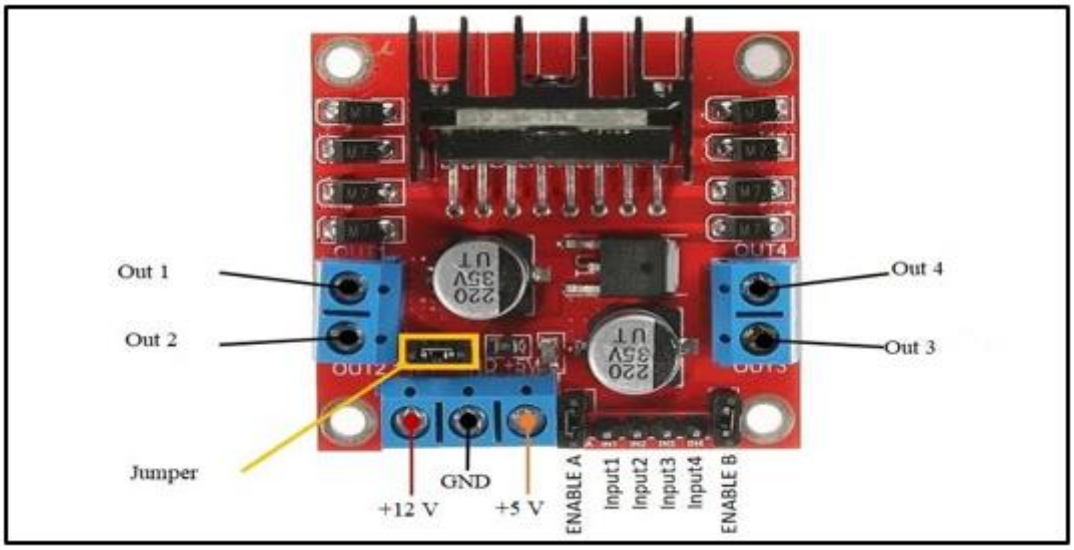

Figure 3.3 Motor driver unit[13]

3.3.3. Microcontroller

PIC12F675 is a microcontroller designed for low end applications and systems. It is good for learning and experimenting for engineers because it has high flash memory rewrite cycle. The controller has 2KBytes flash memory which is enough for starters to develop basic programs. Also the 6 GPIO pins are designed for handling a maximum current of 25mA which meets the threshold

of many peripheral devices and sensors[14]. The schematic diagram of the circuit for the microcontroller shown in figure 3.4.

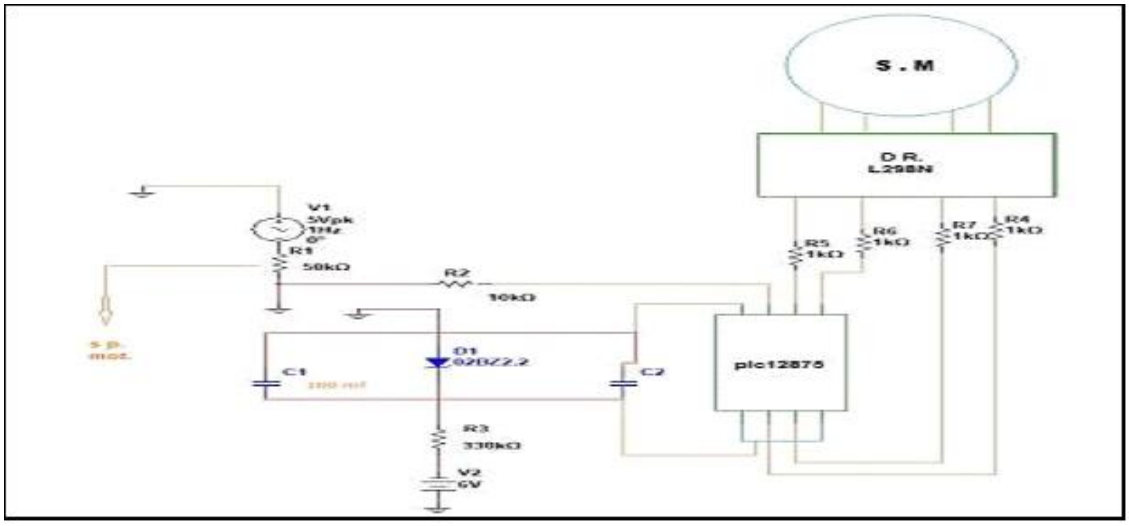

Figure 3.4 schematic diagram of the circuit for the microcontroller.

3.3.4 Stepper motor

Bipolar Nema 23 stepper motor with 1.8 deg. step angle (200 steps/revolution). Each phase draws 2.8A, allowing for a holding torque of 1.26Nm (178.5oz.in). With electrical specification: type: bipolar stepper step angle: 1.8 deg, holding torque: 1.26Nm (178.5oz.in), rated current/phase: 2.8A, phase resistance: 0.9ohms, and inductance: 2.5mH+/-20 %(1KHz)[15]. Figure 3.5 shown the stepper motor and the way to control it. Also, figure 3.6 shown the inlet and the outlet of the motor. The datasheet shown in Appendix B.

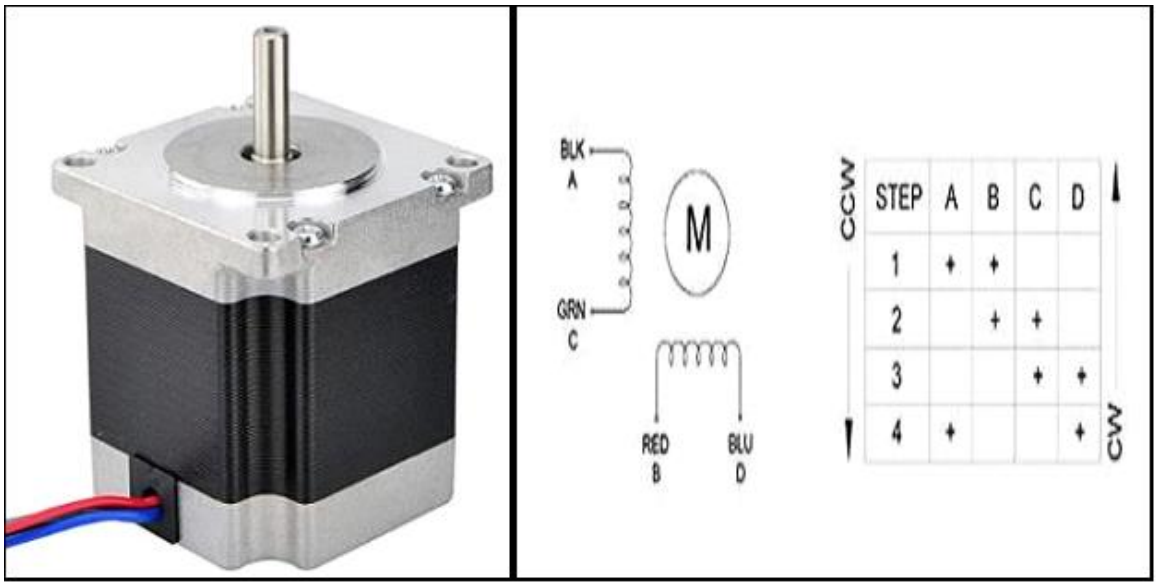

Figure 3.5 shown the stepper motor and the way to control it [25].

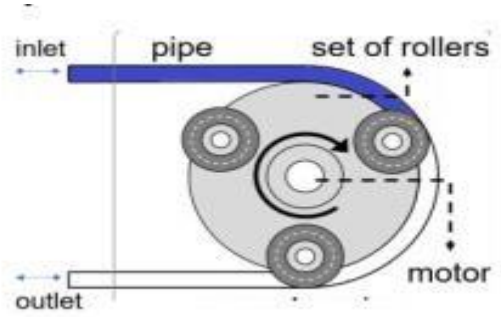

Figure 3.6 inlet and the outlet of the motor.

3.4 software configuration

The flow code is perfect for low cost entry into PIC-micro development. And is fully compatible with the range of E-block accessories. The great advantage of Flow code is that it allows those with little to no programming experience to create complex electronic systems in minutes. This bundle consists of a copy of Flow code, a USB PIC-micro microcontroller multi-programmer, an LED E-block (8 leds), a switch Eblock (8 switches), an LCD E-block (2 line 16 character) and a USB cable, power supply. It is ideal for rapid project development[16]. Figure 3.7 shown the flow code the main site of the program.

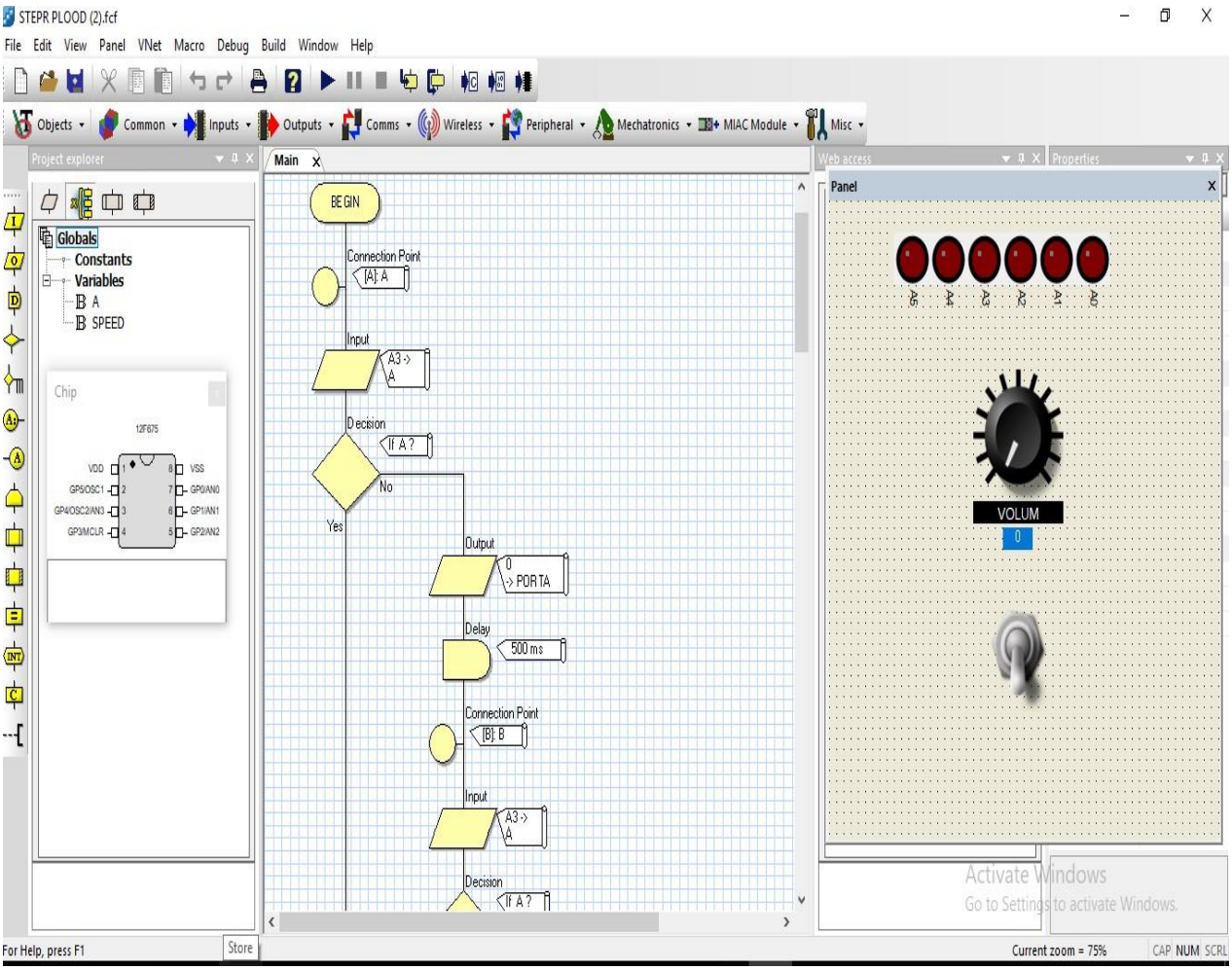

Figure 3.7 flow code the main site of the program.

3.5 System Algorithm

The system is work when the power is ON so the motor is working according to the select speed. So, if there is a bubble in the tube that contain the fluid (blood) the motor automatically is OFF by the safety unit the build in the system according to the program that built in the microcontroller with flow code software. Figure 3.8 illustrate the algorithm for the system.

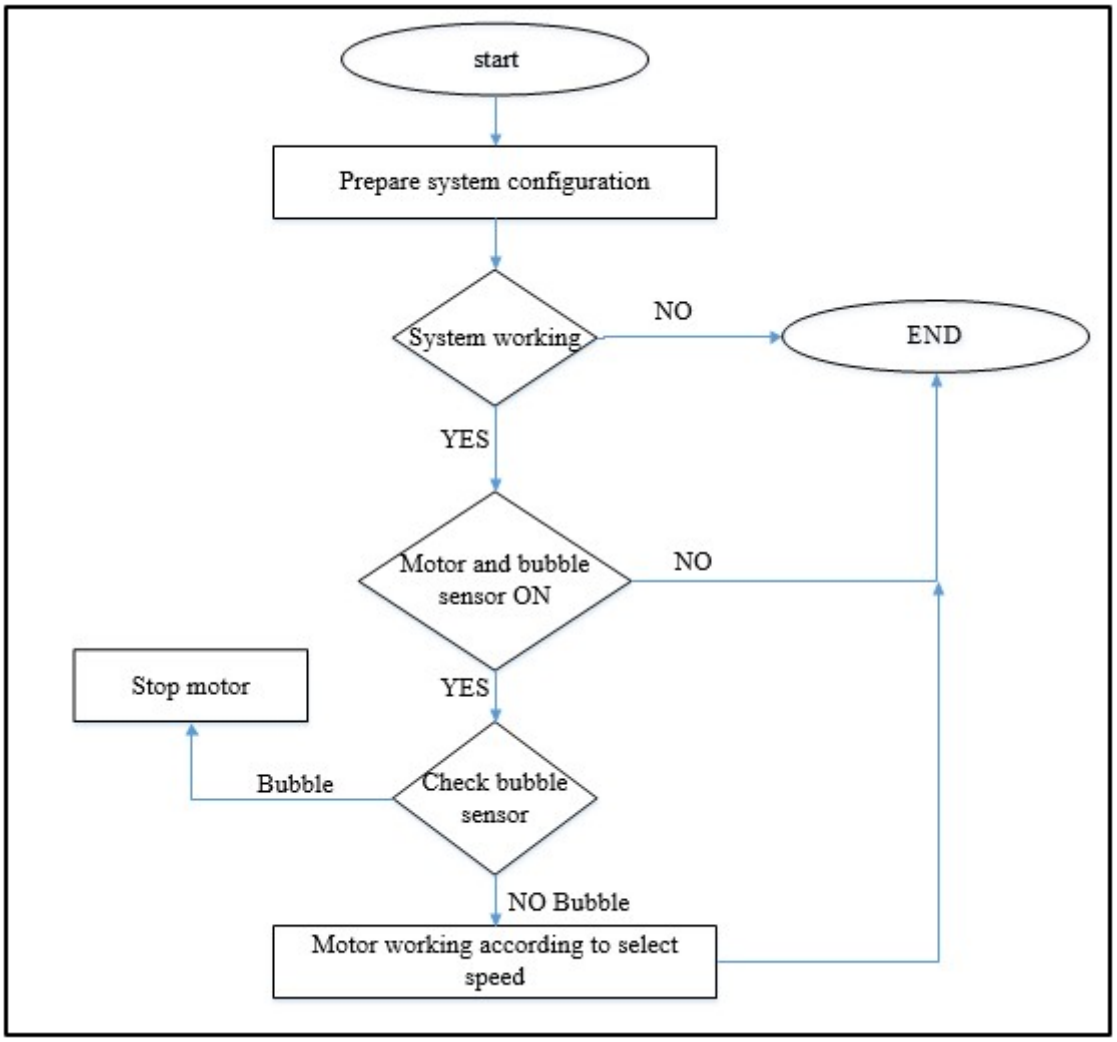

Figure 3.8 algorithm for the system.

3.7 Performance Classification

The performance classification of the system has been derived from three statistical analyses, namely, sensitivity, specificity, and accuracy [17, 18]. These measurements are based on four indices that have four possible attempts, which are: the true positive (*TP*) is the motor is ON and the bubble sensor is active, false positive (*FP*) is the motor is OFF and the bubble sensor is active, true negative (*TN*) is the motor is ON and the bubble sensor is not active, and false negative (*FN*) is the motor is OFF and the bubble sensor is not active. Sensitivity (*SN*) refers to the ability of the system to perform the function of the system (the sensitivity is also known as a recall), as shown in Equation (3.1) [17].

$$SN.\,\% = \frac{TP}{TP + FN} \times 100 \tag{3.1}$$

Specificity (*SP*) refers to the ability of the function of the system, as shown in Equation [27]. (3.2)

$$SP.\,\% = \frac{TN}{TN + FP} \times 100 \tag{3.2}$$

Accuracy (*AC*) refers to the overall ability of the function of the system, as shown in Equation (3.3) [17].

$$AC.\,\% = \frac{TP+TN}{Pn+Nn} \times 100 \quad (3.3)$$

where *Pn* and *Nn* denote the number of positive and negative attempts, respectively.

Likewise, for evaluating the overall system, F-measure accuracy (overall accuracy) has been computed to evaluate the overall performance [19]. F-measure accuracy represents the combination of recall (sensitivity) and precision, which is defined, as follows:

$$Precision\,\% = \frac{TP}{TP + FP} \times 100 \quad (3.4)$$

$$F - measure\ accuracy\,\% = 2 \times \frac{recall \times precision}{recall + precision} \times 100 \quad (3.5)$$

CHAPTER 4 RESULTS AND DISCUSSION

4.1 Introduction

In this chapter, the results of the methodology are presented in two phases, namely, safety unit to protect the peristaltic pump in diagnosis and heart-lung machines from bubbles and performance evaluation of the system. Moreover, validated measurements of the proposed system are investigated statistically (i.e., accuracy, sensitivity, and specificity).

4.2 Roller effect

This section indicates the effect of the roller and the diameter of the tube which is illustrated in Figure 4.1. It demonstrates the various type of tube and see the effect for the follow of the fluid.

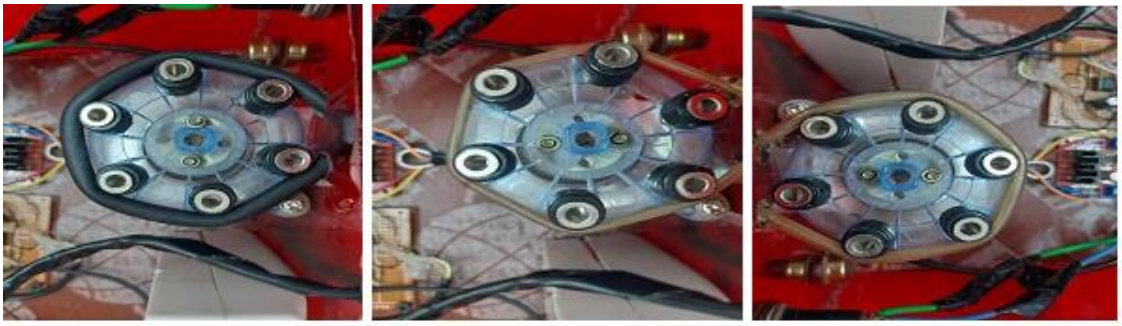

Figure 4.1 demonstrates the effect of the diameter tube

4.3 Performance Results of the system

In this section, the performance results of the system can be discussed below:

The classification models (true positive [TP], false positive [FP], true negative [TN], and false negative [FN]) are evaluated. These classification models are, illustrated in Tables 4.1 to 4.2. All test cases are carried out by repeating for many attempts.

Table 4.1 Experimental evaluation for test 1

Test 1	Speed 1	Speed 2
attempts	100	200
TP	99	198
FN	1	2
Sensitivity (%)	99	99

Table 4.2 Experimental evaluation for test 1

Test 2	Speed 1	Speed 2
attempts	200	300
TN	199	299
FP	1	1
Specificity (%)	99.5	99.6

Table 4.1 and Table 4.2 shows the experimental evaluations. Accuracy, sensitivity, and specificity are statistically analyzed to validate the performance of the proposed system. These statistical analyses are measured according to Equations (3.1–3.3) (Chapter 3). The average sensitivity, specificity, and accuracy for the test one are 99%, 99.55%, and 99.33%, respectively.

Table 4.3 indicates the overall performance accuracy information of the system. The accuracy validation is expressed as a confusion matrix. The confusion matrix gives a clear illustration of the number of experiments and the accuracy of the system. There are 50 numbers of experiments for the total system. The experiments are implemented by collecting 50 trials and measure the value of accuracy from the confusion matrix. The overall accuracy of the WCS is determined from Equations (3.4-3.5) (Chapter three). The overall evaluation accuracy is estimated to be ≈98%.

Table 4.3 Overall accuracy of the system

Parameters	Test 1	Test 2
Total number of experiment	100	100
TP	96	97
FP	1	1
TN	2	1
FN	1	1
Confusion matrix= $TP \quad FN$ $FP \quad TN$	Confusion matrix= 96 1 1 2	Confusion matrix= 97 1 1 1
Precision (%)	98.9	98.9
Recall (%)	98.9	98.9
WCS accuracy = $2 \times \frac{recall + precision}{recall * precision} \times 100$ %	98.9	98.9
Overall Accuracy = 98.9 %		

CHAPTER 5 CONCLUSIONS AND RECOMMENDATIONS

High power, high current, high stability, safe and cost-effective of 5VDC 4A DC power supply of project system is introduced multiple protections of over-current and short-circuit. L298N motors is continue to move in the absence of bubbles and will be Off in the presence of bubble in the tube return to move again if the bubble is removed. PIC12F675 microcontroller which is enough for to develop basic programs by starter. The controlling on pump speed and motor Off in case of bubble presence, all these are performed by PIC12F675 microcontroller. The proposed design of pump and fabricated model has ability to pump liquid with high sensitivity and accuracy. For future work it is expected that increasing in number of roller will increase streamlining of the liquid flow and reduce possibility of air bubble insertion.

REFERENCES

1. F. Esser, F. Krüger, T. Masselter, and T. Speck, "Characterization of biomimetic peristaltic pumping system based on flexible silicone soft robotic actuators as an alternative for technical pumps," in *Conference on Biomimetic and Biohybrid Systems*, 2019, pp. 101-113.
2. S. C. Gasoto, B. Schneider Jr, and J. A. Setti, "Study of the Pulse of Peristaltic Pumps for Use in 3D Extrusion Bioprinting," *ACS omega,* vol. 7, pp. 2409124101, 2022.
3. T. Zehetbauer, A. Plöckinger, C. Emminger, and U. D. Çakmak, "Mechanical design and performance analyses of a rubber-based peristaltic micro-dosing pump," in *Actuators*, 2021, p. 198.
4. Y. Zhou, B. Sun, M. Chen, and C. Cui, "Research of flow dynamics and occlusion condition in roller pump systems used for ventricular assist," *Artificial Organs,* vol. 45, pp. E1-E13, 2021.
5. I. Tamadon, V. Simoni, V. Iacovacci, F. Vistoli, L. Ricotti, and A. Menciassi, "Miniaturized peristaltic rotary pump for non-continuous drug dosing," in *2019 41st Annual International Conference of the IEEE Engineering in Medicine and Biology Society (EMBC)*, 2019, pp. 5522-5526.
6. M. R. Behrens, H. C. Fuller, E. R. Swist, J. Wu, M. Islam, Z. Long*, et al.*, "Open-source, 3D-printed peristaltic pumps for small volume point-of-care liquid handling," *Scientific reports,* vol. 10, pp. 1-10, 2020.
7. S. Pech, R. Richter, and J. Lienig, "Peristaltic Pump with Continuous Flow and Programmable Flow Pulsation," in *2020 IEEE 8th Electronics SystemIntegration Technology Conference (ESTC)*, 2020, pp. 1-5.
8. M. Mirzaei and A. M. Parrany, "An experimental study on real–time analysis of two–phase peristaltic slug flows in dialysis machines," *Flow Measurement and Instrumentation,* vol. 79, p. 101941, 2021.
9. M. P. McIntyre, G. van Schoor, K. R. Uren, and C. P. Kloppers, "Modelling the pulsatile flow rate and pressure response of a roller-type peristaltic pump," *Sensors and Actuators A: Physical,* vol. 325, p. 112708, 2021.
10. G. Formato, R. Romano, A. Formato, J. Sorvari, T. Koiranen, A. Pellegrino*, et al.*, "Fluid–structure interaction modeling applied to peristaltic pump flow simulations," *Machines,* vol. 7, p. 50, 2019.
11. J. Falcão Carneiro, J. B. Pinto, F. Gomes de Almeida, and M. Fateri, "Model and Experimental Characteristics of a Pneumatic Linear Peristaltic Actuator," *Information,* vol. 11, p. 76, 2020.
12. https://www.amazon.com/seeed-studio-Switching-Supply-
13. Jetson/dp/B07WRK9QRD/ref=sr_1_16?dchild=1&keywords=Computer%2 BPower%2BSupplies%2B5v&qid=1623347770&s=pc&sr=1-16&th=1. [13] https://www.amazon.com/Qunqi-Controller-Module-StepperArduino/dp/B014KMHSW6.
14. https://components101.com/microcontrollers/pic12f675-pinout-datasheet.
15. https://www.amazon.com/STEPPERONLINE-Stepper-Motor-179ozBipolar/dp/B00QG1ZF48/ref=sr_1_10?crid=23GWHNF6E9LXY&dchild=1 &keywords=stepper+motor+kit&qid=1623350488&sprefix=stepper+motor+ %2Caps%2C-1&sr=8-10.
16. https://flowcode.software.informer.com/4.0/.
17. G. Kucukyildiz, H. Ocak, S. Karakaya, and O. Sayli, "Design and implementation of a multi sensor based brain computer interface for a robotic wheelchair," *Journal of Intelligent & Robotic Systems,* vol. 87, pp. 247-263, 2017.

18. H. F. Jameel, S. L. Mohammed, and S. K. Gharghan, "ElectroencephalographBased Wheelchair Controlling System for the People with Motor Disability Using Advanced BrainWear," in *2019 12th International Conference on Developments in eSystems Engineering (DeSE)*, 2019, pp. 843-848.

19. C. Ma, W. Li, R. Gravina, and G. Fortino, "Posture detection based on smart cushion for wheelchair users," *Sensors,* vol. 17, p. 719, 2017.